A log-linear model of grain size influence on the geochemistry of sediments

H. v. Eynatten and R. Tolosana-Delgado

Dept. of Sedimentology and Environmental Geology, Geoscience Center, University of Göttingen, Germany; *hilmar.von.eynatten@geo.uni-goettingen.de*

Abstract

Sediment composition is mainly controlled by the nature of the source rock(s), and chemical (weathering) and physical processes (mechanical crushing, abrasion, hydrodynamic sorting) during alteration and transport. Although the factors controlling these processes are conceptually well understood, detailed quantification of compositional changes induced by a single process are rare, as are examples where the effects of several processes can be distinguished. The present study was designed to characterize the role of mechanical crushing and sorting in the absence of chemical weathering. Twenty sediment samples were taken from Alpine glaciers that erode almost pure granitoid lithologies. For each sample, 11 grain-size fractions from granules to clay (ϕ grades <-1 to >9) were separated, and each fraction was analysed for its chemical composition.

The presence of clear steps in the box-plots of all parts (in adequate ilr and clr scales) against ϕ is assumed to be explained by typical crystal size ranges for the relevant mineral phases. These scatter plots and the biplot suggest a splitting of the full grain size range into three groups: coarser than $\phi=4$ (comparatively rich in SiO_2, Na_2O, K_2O, Al_2O_3, and dominated by "felsic" minerals like quartz and feldspar), finer than $\phi=8$ (comparatively rich in TiO_2, MnO, MgO, Fe_2O_3, mostly related to "mafic" sheet silicates like biotite and chlorite), and intermediate grains sizes ($4 \leq \phi < 8$; comparatively rich in P_2O_5 and CaO, related to apatite, some feldspar).

To further test the absence of chemical weathering, the observed compositions were regressed against three explanatory variables: a trend on grain size in ϕ scale, a step function for $\phi \geq 4$, and another for $\phi \geq 8$. The original hypothesis was that the trend could be identified with weathering effects, whereas each step function would highlight those minerals with biggest characteristic size at its lower end. Results suggest that this assumption is reasonable for the step function, but that besides weathering some other factors (different mechanical behavior of minerals) have also an important contribution to the trend.

Key words: sediment, geochemistry, grain size, regression, step function

1 Introduction

Numerical modeling has become a powerful and versatile tool in several fields of theoretical and applied geosciences during the last decades. In the field of sedimentology and basin analysis, such modeling usually comprise basin subsidence (and possibly inversion), heat and fluid flow, basin fill (stratigraphic modeling) as well as climatic, oceanographic and biological forcing of sedimentary systems (e.g, Harbaugh and others, 1999; Harff and others, 1999). Basin-fill models, for example, are strongly controlled by sediment supply, subsidence and sea-level fluctuations. They are mostly designed to predict or reconstruct sediment distribution (sedimentation rates in space and time) under known boundary conditions (e.g., Storms and Swift, 2003), and may include some rough information on basic lithologies (carbonates, evaporates, fine vs. coarse-grained clastics, etc.). Other models focus on sediment transport (e.g., Bobertz and others, 2005) or diagenetic modeling (e.g., Walderhaug, 2000). Compared to these quite detailed models, little has been done so far concerning a comprehensive numerical-statistical model for describing the composition of clastic sediments, i.e. their grain size, mineralogy, and/or geochemistry.

The mineralogical and geochemical composition of sediments and sedimentary rocks is controlled by a range of factors from the composition of the source rocks to all the processes that modify the material coming from the source rocks such as chemical weathering (depending on climate and relief), mechanical crushing and abrasion during transport of the sediment from source to sink, grain-size fractionation due to hydrodynamic sorting, and the specific conditions of the depositional environment (e.g., Pettijohn and others, 1987; Weltje and von Eynatten, 2004). Therefore, modeling sediment composition requires good knowledge of the source rocks and of the way and degree the various modifying processes were active.

Although the general scheme of the influences of the controlling factors on sediment composition appears to be well understood, detailed investigations of compositional changes induced by a single process are rare, because (i) data from natural systems are mostly ambiguous due to the complexity of separating chemical from physical effects (Johnsson, 1993), and (ii) laboratory data are almost non-existent due to the limitations of time. Therefore it needs investigations from natural laboratories where sediment generation is largely controlled by a single process, for example, chemical weathering or mechanical crushing (comminution). Whereas chemical weathering in general has received high attention (e.g., Lovering, 1959; Nesbitt and Wilson, 1992; Nesbitt and Markovics 1997; Ohta and Arai, 2007) there is especially a lack of information on the effects of some physical processes on sediment formation (Nesbitt and Young 1996). Physical processes generally include in-situ disintegration (e.g., rock fracturing and loosening of grains by changes in temperature and frost action), crushing (comminution by mechanical forces such as shear stresses at the base of glaciers), and mechanical abrasion or attrition (e.g. Blatt and others, 1972). Finally, hydrodynamic sorting separates the detrital material according to its grain size, shape, and density.

In this paper, we use chemical data from twenty sediment samples that were taken from three retreating Alpine glaciers of the Aar Massif in central Switzerland. Samples range from fine-grained clay to coarse-grained granules. Our hypothesis is that these sediments were not affected by chemical weathering and, thus, physical comminution and subsequent hydrodynamic sorting exclusively control the composition of these sediments. A log-linear regression model is used to describe the compositional changes over the full grain size range. We further test the hypothesis of the absence of chemical weathering by comparing the observed compositional changes versus well-defined trends of chemical weathering known from the literature (e.g., Nesbitt and Markovics, 1997; von Eynatten and others, 2003; Ohta and Arai, 2007).
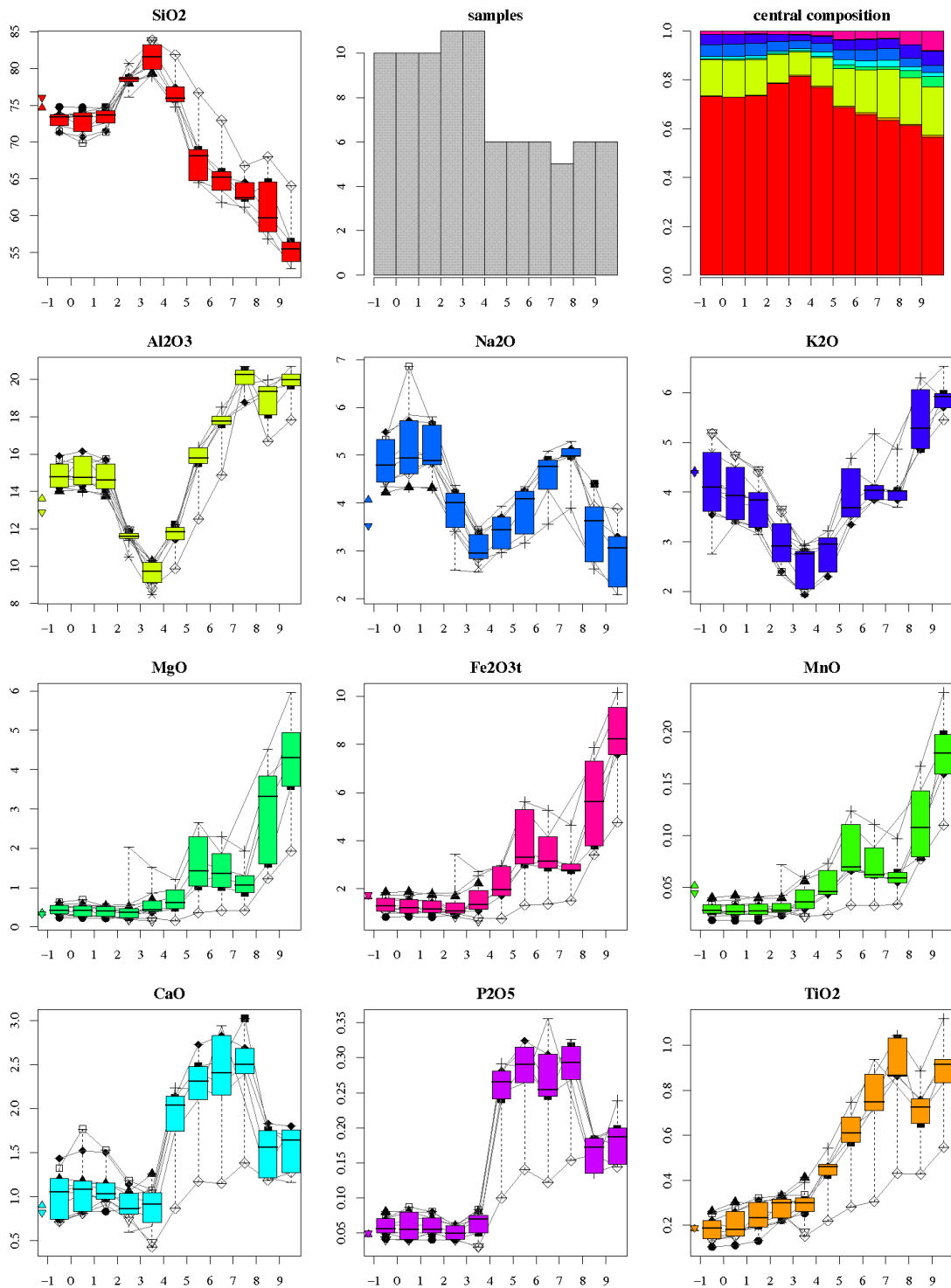
Figure 1: Box-plots of the observed composition as a function of grain size (accessorily, symbols represent samples according to the legend in Figure 5). The number of samples for each grain size fraction, and their (geometric) averages are also displayed. Colours of the averages bars follow the legend in the box-plots. In these, several order statistics are represented (minimum and maximum as extremes of the wiskers, the boxes themselves enclose the 25-75% range of the data, and the central line is the median) for each grain size. Finally, below -1 we include the (geometric) average composition of hand rock specimens (triangle down) and of the bedrock (triangle up) reported by Debon and Lemmet (1999).

2 Data Base

The samples were collected from moraines and glacio-fluvial deposits from the Rhone, Damma and Tiefer Glaciers (Cantons of Valais, Uri and Schwyz, Switzerland). All these glaciers drain and erode almost pure granitoid lithologies (granites, granodiorites, orthogneisses, etc.) from the so-called central Aar granite (Aar massif, Central Alps). According to the compilation by Debon and Lemmet (1999), the mineral modal composition of the granitoids varies from quartz 21-35%, feldspar 61-65% and mafics 1-14%. The monzogranites and granodiorites of the Central Aar granite s.str. exhibit a narrow range (quartz 30-34%, feldspar 58-66%, mafics 4-8%). Characteristic mafic and accessory minerals are biotite, garnet, titanite, allanite (epidote group), and sometimes fluorite.

Twenty sediment samples and eight cobbles that reflect the primary source rocks were taken from the glacial deposits, either close to the front of the retreating glacier tongue or from side moraines. The sediments were separated into eleven grain-size fractions ranging from $\phi \leq$-1 to ϕ >9 (from granules to clay grade) by sieving and centrifuge-aided settling. Grain size distributions were measured by both laser granulometry of the bulk sample and by weighing the individual grain-size fractions of each sample. Each cobble and each sediment grain-size fraction was powdered, fused using lithium metaborate, and subsequently analysed using X-ray fluorescence for major oxides (SiO_2, Al_2O_3, TiO_2, total Fe as Fe_2O_3, MnO, MgO, CaO, Na_2O, K_2O, P_2O_5) , and several trace elements (Ba, Co, Cr, Cu, Ga, Nb, Ni, Pb, Rb, Sc, Sr, V, Y, Zn, Zr, Nd). In this contribution, only the major oxide composition is studied individually for each grain size category, without using the grain size distribution curves to bind them. Figure 1 shows a box-plot representation of the raw variables in the analyzed data set.

3 Methods

3.1 Brief summary of geometry of compositions

A *composition* is a *row vector* $\mathbf{x}$=[x_1, x_2, ..., x_D] of positive components carrying only relative information, i.e. scaling it by a non-negative constant does not change its meaning. For this reason, compositions are typically applied the *closure operation* $C(\cdot)$—that is, rescaled to sum up to 100%—without losing any relevant information. The set of compositions of D parts is called the D-part *simplex*, denoted S^D. A *subcomposition* is just the closure of any subset of 2 or more parts of a composition, and it plays the role that marginals do with conventional vectors. The simplex can be given a Euclidean space structure, by the three operations of perturbation ($\oplus$), powering ($\odot$) and Aitchison scalar product ($<\cdot,\cdot>_A$), respectively playing the roles of translation (addition), scaling (multiplication by a scalar), and Euclidean scalar product (inner product or projection). The original definitions of these operations can be found in Aitchison (1986, 1997, 2002), and the proofs that they indeed build an Euclidean space structre can be found in Billheimer and others (2001) or Pawlowsky-Glahn and Egozcue (2001). These operations can be re-expressed as conventional addition, multiplication and inner product by the so-called *centered log-ratio* transformation of Aitchison (1986),

$$\mathrm{clr}_i(\mathbf{x}) = \ln(x_i) - 1/D \cdot \Sigma_j \ln(x_j).$$

This operation is an *isometry*, i.e. $\mathrm{clr}(\mathbf{x} \oplus \lambda \odot \mathbf{y})$=$\mathrm{clr}(\mathbf{x})+\lambda \cdot \mathrm{clr}(\mathbf{y})$ and $<\mathbf{x},\mathbf{y}>_A = \mathrm{clr}(\mathbf{x}) \cdot \mathrm{clr}^t(\mathbf{y})$, thus largely simplifying further computations (the superindex t means transposition, converting a row vector to a column vector). Note that the inverse clr transformation is the straightforward

$$\mathbf{x} = \boldsymbol{C}[\ \exp(\ \mathrm{clr}\,(\mathbf{x}) \ ) \ ],$$

where the exponential is applied component-wise.

3.2 Review of compositional statistics

To compute an average compatible with that structure, Aitchison (1986) proposed to take the closed geometric mean of the parts, which is equivalent to the *inverse clr* transformation of the *average* of the *clr-transformed values*,

$$\mathbf{m} = \mathrm{clr}^{-1}(\ 1/\mathrm{N} \cdot \Sigma_n \ \mathrm{clr}(\boldsymbol{x}_n) \ ).$$

This is the average used in this paper (e.g. in Figs. 1 and 3). Regarding the variance-covariance structure of a compositional data set, there are several ways to express it in a compatible way (Aitchison, 1986, 1997, Pawlowsky-Glahn and Egozcue, 2002, and Pawlowsky-Glahn, 2003). In our case, we are only interested in a way to represent it graphically, namely the *compositional biplot*.

The clr transformation helped Aitchison (1997, 2002) to define a *compositional biplot*, this is, an optimal bi-dimensional joint representation of the data samples and variables. It is based on a singular value decomposition (SVD) of the data set, *after* clr transformation and centering. Recall that in a compositional biplot, clr-transformed parts are represented as arrows, and each sample as a point. In such a biplot, a link between any two variables represent their log-ratio: orthogonal links suggest uncorrelated pairs of log-ratios, parallel links suggest well-correlated pairs of log-ratios; a short link suggests that its two parts are quasi-proportional or highly correlated, and a long link suggest that the two parts could be unrelated (although this should be taken as just a hint). Rays should not be analyzed, as they represent the clr transformed parts, which have non-intuitive one-to-many relationships with the original parts.

3.3 Linear compositional models

Thanks to the compositional operations of section 3.1, a *compositional linear trend* completely embedded in the simplex, can be defined as (e.g. Daunis-i-Estadella and others, 2002):

$$\mathbf{z}(t_1, \ ..., \ t_s) = \mathbf{b}_0 \oplus t_1 \odot \mathbf{b}_1 \oplus \cdots \oplus t_s \odot \mathbf{b}_s \oplus \mathbf{e}(\phi) \qquad (1)$$

Here $\{t_1, \ ..., \ t_s\}$ can be any *real* variables, $\mathbf{b}_0$ represents a starting composition, $\{\mathbf{b}_1, \ ..., \ \mathbf{b}_s\}$ are vectors of change, and $\mathbf{z}(t_1, \ ..., \ t_s)$ is the resulting composition. This is particularly suited to regression problems: let $\mathbf{z}$ be a compositional variable which we want to explain as a function of $\{t_1, \ ..., \ t_s\}$, a set of explanatory variables (time, depth, grain size, etc.). Let then $\mathbf{T}$ be a matrix containing a first column full of ones, and the rest with all explanatory variables by columns: in this matrix, each row represents an observation and each column a variable. Likewise, let $\mathrm{clr}(\mathbf{X})$ contain the clr-transformed compositions, where each row gives a clr-transformed sample. Then multiple regression (e.g., Mardia and others, 1979) provides as estimate of the coefficients

$$\mathrm{clr}(\mathbf{B}) = (\mathbf{T}^t \cdot \mathbf{T})^{-1} \cdot \mathbf{T}^t \cdot \mathrm{clr}(\mathbf{X})$$

for the vectors of change, where each compositional vector $\mathbf{b}_i$ is in a row of $\mathbf{B}$.

3.4 Weathering indexes based on a compositional geometry

These compositional techniques have been used to derive two indices of weathering. Working with principal components (SVD), von Eynatten and others (2003) derived an index of weathering alternative to the CIA (*chemical index of alteration*, Nesbitt and Young 1984), which is optimal for feldspar weathering but does not adequately capture other effects. As CIA, von Eynatten and others (2003) index is defined using just the subcomposition (CaO^*+N_2O) vs. K_2O vs. A_2O_3 (CN-K-A) expressed in moles, where $CaO^*=CaO -10/3P_2O_5$ is the reduced Ca-oxide after removing the contribution of apatite. These authors estimated the weathering direction as $\mathbf{b}_t=[0.13, 0.34, 0.53]$. Ohta and Arai (2007) took the approach one step further, working with the composition of SiO_2, Al_2O_3, TiO_2, total Fe as Fe_2O_3, MgO, CaO^* (reduced for apatite), Na_2O and K_2O. They collected from several references a data set of weathering profiles on several types of rocks together with well-established standard analysis of fresh specimens of the most important igneous rocks on Earth, and identified the first principal component (of a SVD) as a global direction of weathering. Table 1 contains an expression of the coefficients of these two weathering indexes, normalized in a way that enhances comparison with the results exposed in the next section.

4 Results

4.1 Descriptive analysis

The measured chemical compositions of the coarse sand fractions (ϕ between -1 and +1) generally reflect the average composition of source rocks (Fig. 1). Only minor deviations are observed for Al_2O_3, Na_2O, and SiO_2. Note that for all oxides, the averages of rock specimens and reference bedrock are inside the range for the whole grain-size spectrum. In other words, one could obtain the reported rock averages as a mixture of the observed sediment compositions.

With decreasing grain size compositions strongly differ from the initial composition, with some major element oxides showing strongly contrasting patterns, whereas others are very similar. For instance, the pattern of variability of MgO, $Fe_2O_3^{(t)}$, and MnO percentage data with grain size is extremely similar, suggesting that these elements largely derive from the same mineral phase (e.g., biotite). A strong similarity can be also observed between CaO and P_2O_5, suggesting a significant enrichment of apatite in silt fractions (ϕ 4 to 8). As expected, SiO_2 and Al_2O_3 show reverse patterns with a pronounced maximum in SiO_2 (minimum in Al_2O_3) in the very fine sand fraction. Na_2O and K_2O show a largely similar pattern in the sand to coarse silt fractions (up to $\phi=6$). However, towards the finest grades K_2O is strongly increasing (in a similar trend like e.g. MgO) whereas Na_2O decreases again. TiO_2 shows the steadiest increase with decreasing grain size (with an exception at $\phi=8$), and its pattern in the silt to clay fractions is quite similar to Al_2O_3.

Figure 2A shows a general glance of the covariance structure of the whole data set, distinguishing samples according to their grain size. In the major oxide biplot, one can distinguish three groups of elements and of samples: "felsic" elements (K_2O, Al_2O_3, SiO_2, Na_2O) plot together, on the cluster of coarser sediments with code from -1 to 3, and "mafic" elements (MnO, MgO, $Fe_2O_3^{(t)}$) clearly plot on the same direction, together with samples from the finest sediments (8 or 9). Finally, P_2O_5 marks the third pole, where samples of intermediate size with code from 4 to 7 cluster together. Interestingly, CaO plot between P_2O_5 and the felsic group, and TiO_2 between P_2O_5 and the "mafic" group. This disposition supports the hypothesis that grain size controls geochemistry through mineralogy, given that the "felsic" minerals (quartz, feldspars) tend to be coarser than the rest and the highest relative contribution of "mafic" oxides should come from fine-grained biotite and

related sheet silicate minerals. Apatite and some TiO_2 and/or CaO bearing phases are concentrated in an intermediate grains size range (code 4 to 7). A ternary diagram of a representative part of each group is reported in Figure 2B, showing that the grouping presented before is quite homogeneous in this subcomposition. In this case, hard rock samples tend to be similar to the coarse fractions, though there are some with higher Na_2O content (relative to P_2O_5-MgO).

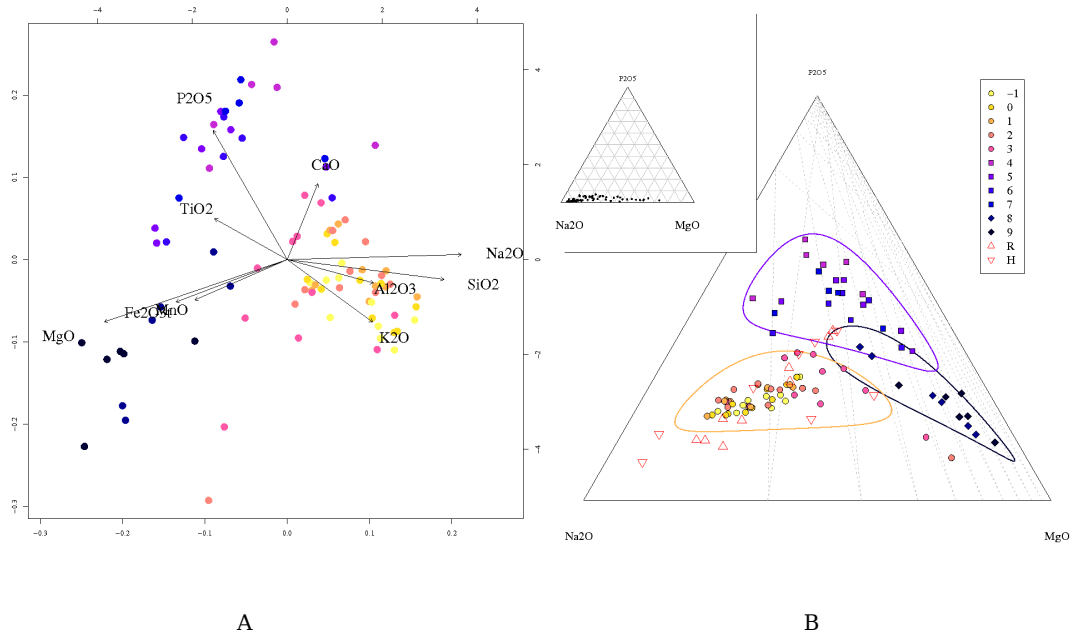A   B

Figure 2: (A) Biplot of major oxide composition, with numbers showing the lower limit of their grain size interval (e.g., 9 means $\phi > 9$). The first principal component (X axis) explains 70.21 % of the total variability, and the second (Y axis) another 18.8 %.
(B) Centered ternary diagram of Na_2O-MgO-P_2O_5, selected from the major oxide biplot to capture approximately the same distribution of samples. Approximate 95% probability regions following Aitchison (1986) are included, for the subcomposition split in three grain fractions: from -1 to 4 ϕ, between 4 and 8 ϕ, and higher than 8 ϕ. This ternary diagram contains as well the composition of rock samples (*H* for our samples, *R* for those of Debon and Lemmet, 1999).

If represented in clr scale, the box-plots of Figure 3 support several of these conclusions. There are fundamentally two types of behaviour of the clr-transformed elements against ϕ. At first glance, it seems that most elements are approximately linearly related with ϕ, either increasing—the "mafics" and TiO_2—, or decreasing—the "felsics"—. But two of them (CaO and P_2O_5) show a quite good step structure, with thresholds in $\phi=4$ and $\phi=8$, and with this in mind, several other seem to have threshold effects: $Fe_2O_3^{(t)}$, for instance, looks quite constant below $\phi=4$, and increases quite linearly afterwards (with the exception of $\phi=8$, where very few samples are available).

A comparison of Figures 1 and 3 allow to highlight several interesting issues. What at first glance could seem as a trend of enrichment for $\phi>3$ of Al_2O_3 at the expense of SiO_2 (Fig. 1) is not appearing in the clr scale, where they are rather proportional. This suggests that the *apparent* enrichment is not related to any alteration process, but due to two facts: that these two elements account together for 80-90% of the total mass and are, thus, prone to the closure effect; and that other silicates tend to crystallize in smaller grains and have higher Al/Si ratios. On the contrary, both scales show strongly similar increasing patterns for $Fe_2O_3^{(t)}$, MnO and MgO, suggesting a genetic relationship between them, confirmed by the biplot (Fig. 2) where they cluster together.
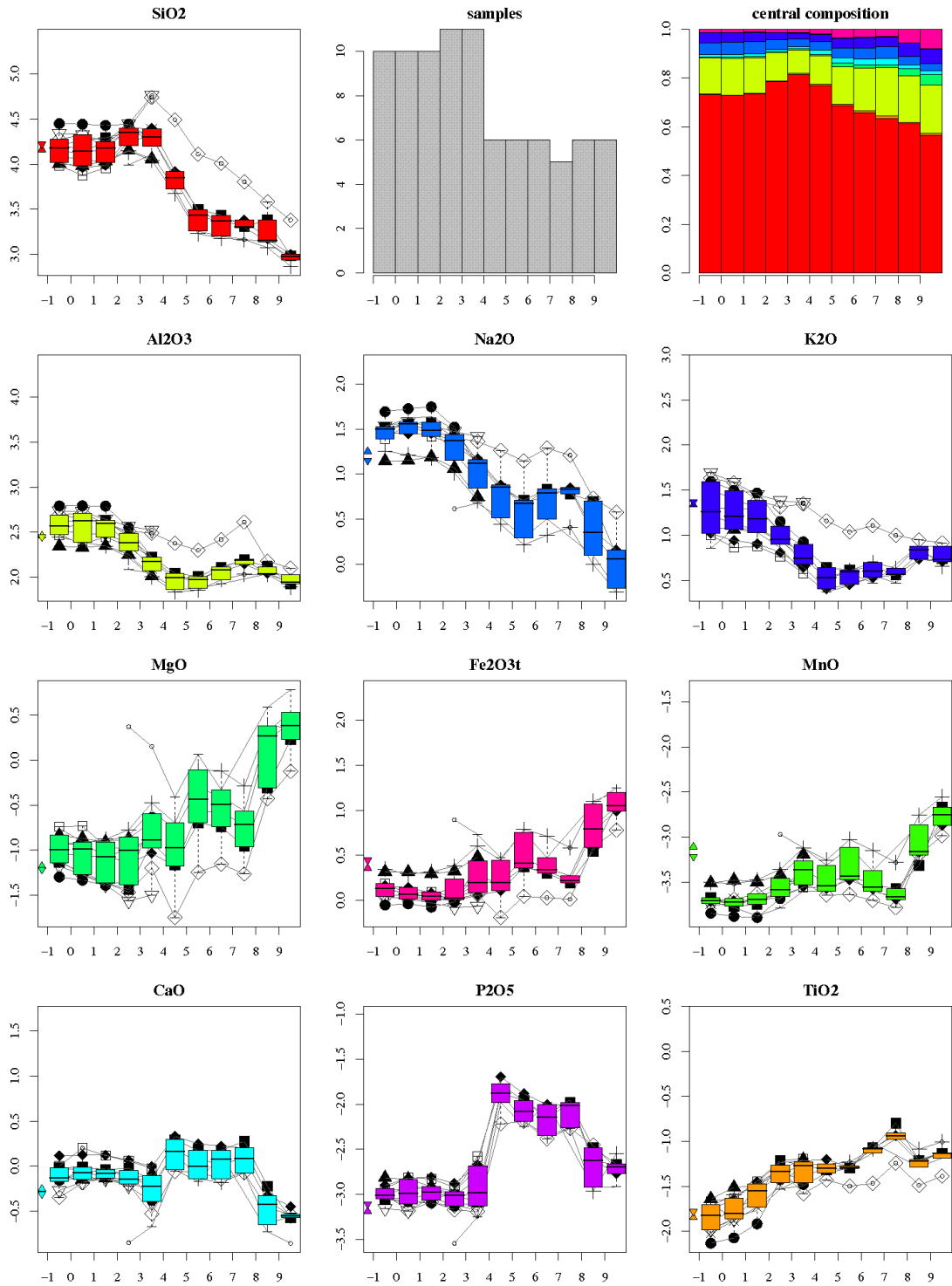
Figure 3: Box-plots of the clr-transformed observed composition as a function of grain size (accessorily, symbols represent samples according to the legend in Figure 5). The number of samples for each grain size fraction, and their back-transformed clr-averages are also displayed. Colors of the averages bars follow the legend in the box-plots. In the box-plots, several order statistics are represented (minimum and maximum as extremes of the whiskers, the boxes themselves enclose the 25-75% range of the data, and the central line is the median) for each grain size. All plots share the same vertical scale span, thus the variability among parts is comparable. Finally, below -1 we include the average composition of the sampled bedrock cobbles (triangle down) and of the bedrock samples (triangle up) reported by Debon and Lemmet (1999).

In summary, the composition of the grain size fractions can be split in three groups with boundaries at $\phi=4$ and $\phi=8$. This discontinuous behavior may be explained as inherited from typical crystal sizes of the major minerals of the source rock. This hypothesis is further explored in the next section.

4.2 Regression analysis: influence of grain size on major oxide composition

The goal here is to *predict* the composition as a function of grain size ϕ. This requires a linear trend [Eq. (1)], which is conveniently recasted into a typical regression problem by means of the clr transformation,

$$\text{clr}_i\,[\mathbf{z}(\phi)] = a_i + b_i \cdot \phi \ + c_i \cdot \text{I}(\phi \geq 4) + d_i \cdot \text{I}(\phi \geq 8) + e_i(\phi),$$

subject to zero sum constraints,

$$\Sigma_i\, a_i = 0, \qquad \Sigma_i\, b_i = 0, \qquad \Sigma_i\, c_i = 0, \qquad \Sigma_i\, d_i = 0, \quad \text{and} \quad \Sigma_i\, e_i(\phi) = 0,$$

the last true for all ϕ. Further, the vector $\mathbf{e}(\phi)$ of the residuals of all parts for a fixed value of ϕ is taken as normally distributed, with zero mean and spread only on the plane orthogonal to the first orthant bisector, $\mathbf{e}(\phi) \sim N^D(\mathbf{0}, \Sigma)$, thus with Σ singular. The step functions $\text{I}(\phi \geq \phi_0)$ are equal to 1 if $\phi \geq \phi_0$, otherwise they are equal to 0.

Results are displayed in Figure 4, showing each clr plot as a function of grain size, and displaying the estimated model. The parameters (regression coefficients) are also displayed, in the form of a bar plot showing the relative weight of each explanatory function (linear dependence, step at $\phi=4$ and step at $\phi=8$). This figure shows that there is no overall Al_2O_3 enrichment (indicative of weathering at these preliminary stages) towards the finer fractions, as the fitted slope is negative. On the other side, the trend is positive for TiO_2 and the "mafic" elements ($Fe_2O_3^{(t)}$, MnO, MgO), which was already explained as the effect of a progressive concentration of biotite and similar feasible mafic minerals in the finer fractions. Nevertheless, K_2O (a major constituent of biotite) does not show a parallel behaviour.

When interpreting compositional trends like this, one should bear in mind that (due to the relative character of compositions) it is not possible to distinguish e.g. between a trend of K_2O depletion keeping Al_2O_3 constant, or a trend of Al_2O_3 enrichment with K_2O constant. Table 1 shows a set of coefficients equivalent to those reported in Figure 4, but which have been forced to be all positive: in other words, assuming no weathering/no depletion of any element mass, these coefficients would produce exactly the same dependence of the composition with grain size. In this representation of the trend, Al_2O_3 is being actually slightly (2.3%) enriched with respect to Na_2O, though the intensity of weathering according to this proxy is minimal when compared with the mafic enrichment (~12-15% in $Fe_2O_3^{(t)}$-MnO-MgO) or TiO_2 (25%). With regard to the first step function coefficients, we can say that the silt fraction is 400% richer in P_2O_5 and 180% in CaO than the finest sand, 100% richer in MgO and $Fe_2O_3^{(t)}$, ~75% in K_2O, Al_2O_3 and MnO, and ~50% in Na_2O and TiO_2, all these assuming SiO_2 unchanged. These values suggest the existence in the characteristic size range of coarse silt of an important source of both P_2O_5 and CaO (most probably apatite), as well as a source of MgO, $Fe_2O_3^{(t)}$, K_2O, Al_2O_3 and MnO (with garnet, biotite, and muscovite being reasonable candidates). Finally, the second step function coefficients suggest a $Fe_2O_3^{(t)}$-MgO source, with a significant contribution of Al_2O_3, K_2O and MnO, to the grain-size

range of finest silt and clay (again biotite and possibly some chlorite are the likely mineral candidates for these elements).

Table 1: Regression coefficients, recast to zero minimum. Due to the properties of the clr transformation, adding a constant to each column of this coefficent matrix does not change the composition we finally predict with them. This particular case was obtained by substracting to each column its lowest value. The second set of columns report the exponential of these values, and represent a multiplicative factor to directly apply to the composition, e.g. passing ϕ=8 the concentration of K_2O and $Fe_2O_3^{(t)}$ are applied a factor of ~3, that of MgO is multiplied by 4, and the MnO concentration by 8/3, whereas P_2O_5 is kept constant. The last two columns give the equivalent compositional directions for the weathering indices of von Eynatten and others (2003) and Ohta and Arai (2007), to be compared with the ϕ column.

	clr coefficients			equivalent composition			indices	
	$I(\phi{>}4)$	$I(\phi{>}8)$	ϕ	$I(\phi{>}4)$	$I(\phi{>}8)$	ϕ	t	W
Si	0.000	0.186	0.082	1.000	1.204	1.085	NA	0.662
Ti	0.448	0.179	0.220	1.566	1.196	1.246	NA	0.809
Al	0.576	0.738	0.023	1.779	2.092	1.023	4.08	1.046
Mn	0.510	0.982	0.144	1.665	2.669	1.155	NA	NA
Mg	0.682	1.370	0.143	1.978	3.936	1.153	NA	0.656
Ca	1.037	0.132	0.046	2.820	1.141	1.047	1.00	0.813
Na	0.458	0.333	0.000	1.580	1.395	1.000	1.00	1.000
K	0.564	1.029	0.001	1.758	2.798	1.001	2.62	0.809
P	1.631	0.000	0.074	5.107	1.000	1.077	NA	NA
Fe	0.676	1.112	0.120	1.966	3.039	1.126	NA	1.470

Discussion

As outlined in the introduction, the framework project of this study has as ultimate goal the development of a comprehensive model of the evolution of the *composition* (abundance of each size and type of grains) of sediments from the source area to the depositional basin. A major goal in the present state of the project is to model the influence of grain size on sediment composition. In this paper the focus is put on the first stages of sediment generation in a glacial mountainous catchment with largely homogeneous felsic crystalline bedrock geology. In such a setting, fluvio-glacial sediments are thought to be largely controlled by comminution and hydrodynamic sorting, with no significant contribution from chemical weathering (Nesbitt and Young, 1996).

Two of the processes that generally exert large control on sediment composition, comminution and chemical weathering, can be distinguished by their imprint on the relation between grain size and geochemistry. *Chemical weathering* should follow linear functions similar to those proposed by von Eynatten and others (2003), or Ohta and Arai (2007). On the contrary, an ensemble of minerals of similar size and mechanical properties undergoing *comminution* should exhibit the same geochemical composition along all the grain size spectrum below their common crystal size. Therefore, assuming that all mineral grains and assemblages in sediments have similar mechanical properties, mechanical crushing (*comminution*) should not largely change the composition of sediments with grain size, except at those ϕ thresholds where a new characteristic crystal size appears: this relationship grain size-composition should thus fundamentally resemble a step-function, reflecting the inherited grain size from the source rocks. Moreover, in the absence of weathering, the geochemical composition should be explained by simple endmember mixture of the typical bedrock minerals. The fit of these two process models was checked, using several geochemical indicators of alteration Ohta and Arai (2007) and compositional data analysis (Aitchison, 1986; Aitchison, 1997: Buccianti and others, 2006).
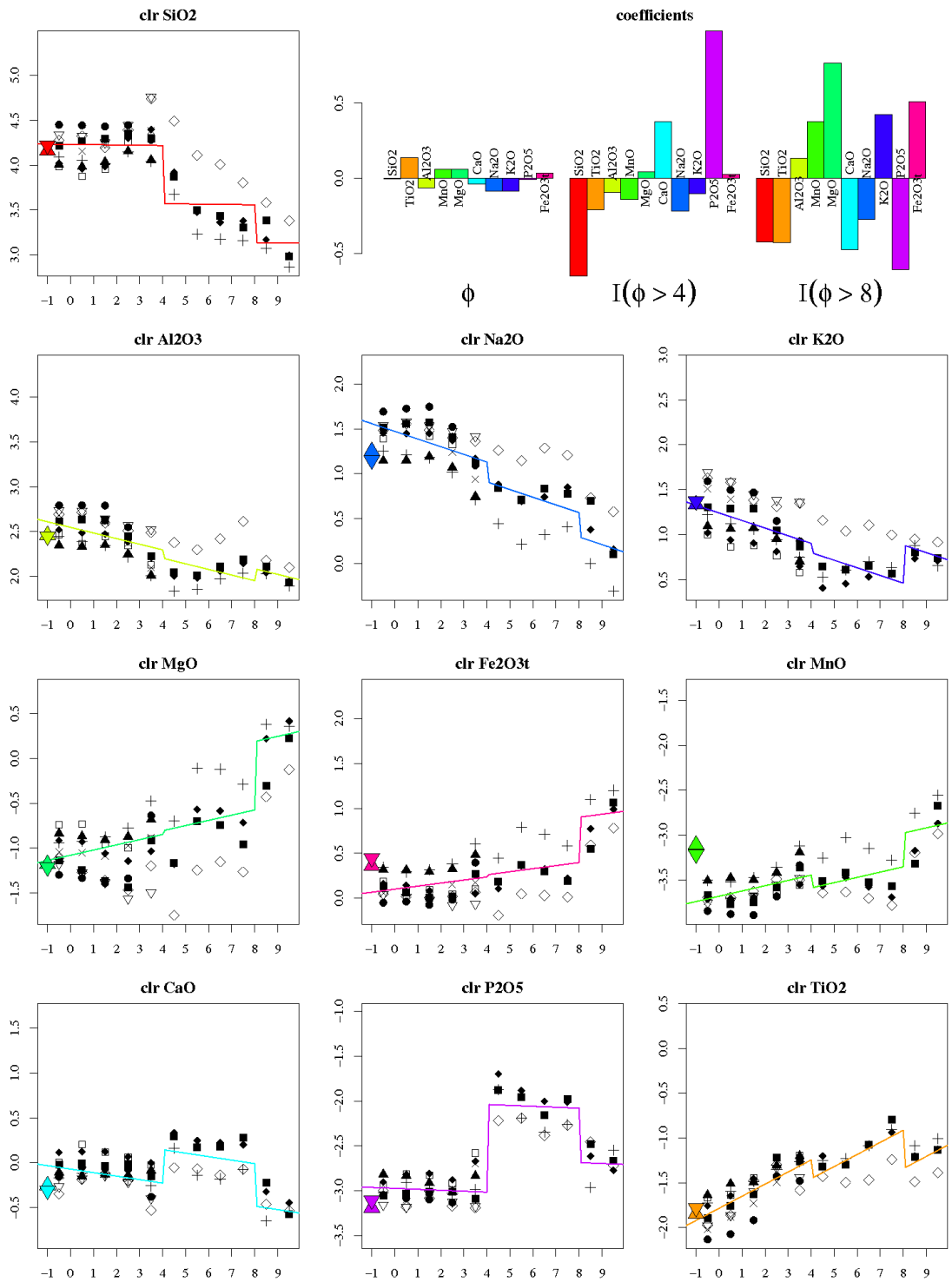
Figure 4: Linear model of explanation of observed clr variability. Each plot reports a clr-transformed part against grain size (black-and-white symbols represent samples according to the legend in Figure 5), together with the fitted model (coloured line) and the composition of reference hand rock samples (coloured triangles: pointing up for references, down for our rock samples). The bar plot represent the coefficients of the 3 explanatory variables.
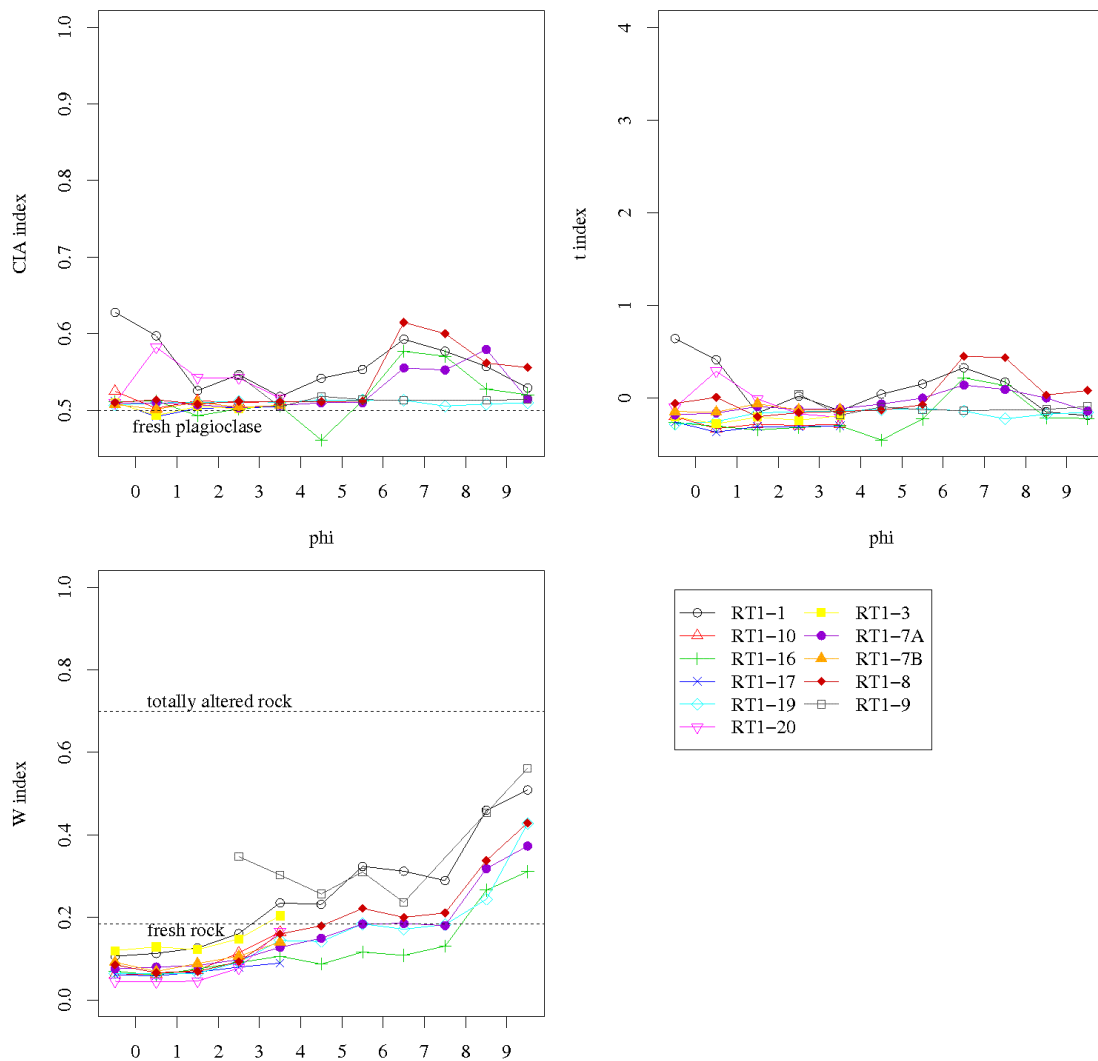
Figure 5: Comparison of existing weathering indexes: CIA index of alteration of feldspar (Nesbitt and Young, 1984), W index (Ohta and Arai, 2007), and projection index t of von Eynatten and others (2003).

The significant steps at ϕ=4 (very fine sand to very coarse silt) and ϕ=8 (fine to very fine silt) observed consistently in percentage raw data (Fig. 1), clr-transformed data (Fig. 3), and highlighted by the log-linear model (Fig. 4), call for a major influence of inherited grain sizes from the source rocks on sediment composition: components with a significant positive step indicate that some related mineral phases massively appear at that size threshold. Consequently, the positive steps observed in the bar plot of Figure 4 suggest the abrupt occurrence (enrichment) of apatite (P_2O_5, CaO) and probably some garnet (MgO, $Fe_2O_3^{(t)}$) from the ϕ=4 fraction on, and biotite ($Fe_2O_3^{(t)}$, MgO, MnO) after ϕ=8. Though other mafic phases (garnet and chlorite) may play a complementary role at this last threshold, the coeval positive step in K_2O underlines biotite predominance among them. Finally, the fact that TiO_2 shows a different behavior at ϕ=8 implies that biotite is not the major Ti-bearing phase in the system.

Apart of the step functions (an effect of pure comminution and inherited crystal sizes), a certain progressive enrichment/depletion trend is visible in several

elements: towards finer fractions, sediments are enriched in mafic elements, and depleted in felsic ones (Fig. 4). Weathering is nevertheless not its most satisfactory explanation for the following reasons. First of all, the "older" (longer exposed) samples (RT1-7A, 7B, 8) do not show depletions in CaO, Na$_2$O or K$_2$O, nor enrichment in Al$_2$O$_3$ (Fig. 4). Furthermore, neither the CIA nor the t-index of von Eynatten and others (2003) do show any trend (Fig. 5). Only the weathering index of Ohta and Arai (2007) showed a slight increase with grain size, compatible with the slight enrichment in Al$_2$O$_3$ against Na$_2$O-K$_2$O in the fitted trend (table 1). Finally, one has to remember that weathering is a process in time, and not in grain size: grain size influence should be an acceleration of weathering itself, as finer fractions offer higher specific surface and should thus be more rapidly altered. In other words, the ϕ trend may be an indicator of the *increase* of weathering intensity in finer fractions, and not the weathering itself.

After considering the possible contribution of weathering in the observed trend as minor, another possible factor is the contrast in mechanical properties (hardness, fissility) of the individual minerals. This has already been invoked to explain why SiO$_2$ (and quartz) is concentrated in the sand fraction. Contrast in hardness between phyllosilicates and the rest of the minerals could explain the constant enrichment trend observed in TiO$_2$, Fe$_2$O$_3^{(t)}$, MnO, MgO as well as K$_2$O for phi > 4 (as seen in Figs. 1-3), being mainly caused by preferential comminution and, thus, enrichment of biotite towards finer grain sizes. This may also explain the increase in the W index for phi >7 because this index includes Fe (and Ti) content as a significant measure of the degree of weathering.

Acknowledgements

References

Aitchison, J. (1986) *The Statistical Analysis of Compositional Data*. Chapman & Hall Ltd., London, reprinted in 2003 with additional material by The Blackburn Press.416 p.

Aitchison, J. (1997). The one-hour course in compositional data analysis or compositional data analysis is simple. In: V. Pawlowsky-Glahn (Ed.), *Proceedings of IAMG'97 – The third annual conference of the International Association for Mathematical Geology*, pp. 3–35. International Center for Numerical Methods in Engineering (CIMNE), Barcelona, 1100 p.

Aitchison, J. (2002). Simplicial inference. In: Viana, M. A. G. and Richards, D. St. P. (Eds.), *Algebraic Methods in Statistics and Probability*, Contemporary Mathematics Series no. 287. American Mathematical Society, Providence, Rhode Island, 340 p.

Billheimer, D., Guttorp, P. and Fagan, W.F. (2001) Statistical interpretation of species composition, *Journal of the American Statistical Association*, 96 (456): 1205–1214.

Bobertz, B., Kuhrts, C., Harff, J.m, Fennel, W., Seifert, I. and Bohling B. (2005) Sediment properties in the western Baltic Sea for use in sediment transport modelling. Journal of Coastal Research, 21: 588-597.

Blatt, H. Middleton, G.V., and Murray, R.C. (1972) *Origin of sedimentary rocks*. Prentice-Hall, Englewood Cliffs, New Jersey, 634 p.

Buccianti, A., Mateu-Figueras, G. and Pawlowsky-Glahn, V. (Eds.) (2006). *Compositional Data Analysis: from theory to practice,* Special Publications no. 264. The Geological Society, London.

Daunis-i-Estadella, J. Egozcue, J.J. and Pawlowsky-Glahn, V. (2002) Least squares regression in the Simplex. In: Bayer, U., Burger, H. and Skala, W. (Eds) *Proceedings of IAMG'02 – The eigth annual conference of the International Association for Mathematical Geology*. Selbstverlag der Alfred-Wegener-Stiftung, Berlin, 1106 p. pp 411–416.

Debon, F. and Lemmet, M. (1999). Evolution of Mg/Fe ratios in the Late Variscan plutonic rocks from the External Crystalline Massifs of the Alps (France, Italy, Switzerland). *Journal of Petrology,* 40: 1151–1185. @ARTICLE{EY36,

Eckart, C. and Young, G. (1936) The approximation of one matrix by another of lower rank, *Psychometrika*, 1: 211-218.

Harbaugh, J.W., Watney, W.L., Rankey, E.C., Slingerland, R., Goldstein, R.H. and Franseen, E.K. (1999, Eds). *Numerical experiments in stratigraphy: Recent advances in stratigraphic and sedimentologic computer simulations*, SEPM Spec. Publ., 62, 362 p.

Harff, J., Lemke, W. and Stattegger, K. (1999, Eds.). *Computerized Modeling of Sedimentary Systems*. 452 p., Springer Verlag, Berlin.

Johnsson (1993). The system controlling the composition of clastic sediments. Geological Society of America Special Paper, 284, 1–19.

Lovering, T.S. (1959) Significance of accumulator plants in rock weathering, *GSA Bulletin*, 70: 781–800

Mardia, K.V., Kent, J.T. and Bibby, J.M. (1979) *Multivariate Analysis*. Academic Press, London. 518 p.

Nesbitt H.W. and Wilson, R.E. (1992) Recent Chemical Weathering of Basalts. *American Journal of Science*, 292: 740–777

Nesbitt, H. and G. Young (1984). Prediction of some weathering trends of plutonic and volcanic rocks based on thermodynamic and kinetic considerations. *Geochim. Cosmochim. Acta,* 41: 1523–1534.

Nesbitt, H.W. and Young, G.M. (1996) Petrogenesis of sediments in the absence of chemical weathering: effects of abrasion and sorting on bulk composition and mineralogy. *Sedimentology*, 43: 341–358.

Nesbitt H.W. and Markovics, G. (1997) Weathering of granodioritic crust, long-term storage of elements in weathering profiles, and petrogenesis of siliciclastic sediments. *Geochim. Cosmochim. Acta*, 61: 1653–1670.

Pawlowsky-Glahn and Egozcue (2001) Geometric approach to statistical analysis on the simplex. *Stochastic Environmental Research and Risk Assessment*, 15 (5): 384–398.

Pawlowsky-Glahn and Egozcue (2002) BLU estimators and compositional data. *Mathematical Geology*, 34 (2): 259–274.

Pawlowsky-Glahn (2003) Statistical modelling on coordinates. In Thió-Henestrosa, S. and Martín-Fernández, J.A. (Eds.) *Compositional Data Analysis Workshop – CoDaWork'03, Proceedings*, Universitat de Girona. http://ima.udg.es/Activitats/CoDaWork03/

Ohta T. and Arai, H. (2007) Statistical empirical index of chemical weathering in igneous rocks: A new tool for evaluating the degree of weathering. *Chemical Geology*, 240: 280–297

Pettijohn, F.J., Potter, P.E., Siever, R. (1987) *Sand and Sandstone*. Springer, New York, 553p.

Storms, J.E.A. and Swift, D.J.P. (2003) Shallow-marine sequences as the building blocks of stratigraphy: insights from numerical modelling. *Basin Research*, 15: 287–303.

von Eynatten, H., Barceló-Vidal, C. and Pawlowsky-Glahn, V. (2003). Modelling compositional change: the example of chemical weathering of granitoid rocks. *Mathematical Geology*, 35: 231–251.

Walderhaug, O (2000) Modeling quartz cementation and porosity in Middle Jurassic Brent Group sandstones of the Kvitebjorn field, Northern North Sea. AAPG Bulletin, 84, 1325-1339.

Weltje, G.J. and von Eynatten, H. (2004). Quantitative provenance analysis of sediments: review and outlook. *Sedimentary Geology*, 171: 1–11.

Appendix A: mineral endmember unmixing

A.1   Endmember modeling with generalized inverses and the SVD

This analysis infers a *possible* mineral composition, which accounts for the observed geochemical composition and allow to explain the step structure of its variability. Given known endmembers of *fixed* chemical composition (in a matrix **A**), one can express the observed composition **x** as the classical linear combination of endmembers,

$$\mathbf{x} = \mathbf{y} \cdot \mathbf{A}, \tag{2}$$

with unknown mineral proportions **y** (row vectors). The endmember matrix **A** contains as many column as geochemical parts are available (D), and one row for each endmember, giving the molar weight of each part in that endmember. By definition these columns are compositions, and their sum is irrelevant. Take the number of endmembers as P. There are two main cases:

- one has as many mineral phases as oxides, and no chemical reaction is algebraically possible within the chosen minerals (i.e., the matrix **A** is square and of full rank); then inversion is immediate, as applied by Nesbitt and Young (1996),
- one has different number of unknowns (mineral proportions) and equations (geochemical variables); then one must look for a "best" approximation, for instance via least-squares.

The first case is quite straightforward, as **A** can be directly inverted. If the solution contains negative proportions of minerals, a necessary mineral phase was lost. If the solution is valid, it does not mean that it is true, but just informative, approximate. In the second case, when the number of endmembers is higher than the number of (geochemical) components, there is no single solution: one can either have no solution, or a whole (affine) subspace of them. To find these solutions and choose one of them, we use the following reasoning:

1. Look for $\mathbf{y}_0$ the minimal norm solution, obtained by using generalized inverses on Equation (2). The generalized inverse of **A** is based on its singular value decomposition: this is $\mathbf{A} = \mathbf{U} \cdot \mathbf{D} \cdot \mathbf{V}^t$, where **U** and **V** columns form two different orthonormal sets of vectors in $\mathbf{R}^P$ and $\mathbf{R}^D$ respectively, and **D** is a diagonal matrix, with (D 1) positive elements and ($P{-}D{+}1$) zeroes (we are assuming here $D<P$, thus more mineral endmembers than geochemical components). The matrix $\mathbf{A}^* = \mathbf{V} \cdot \mathbf{D}^* \cdot \mathbf{U}^t$ is the sought generalized inverse, where $\mathbf{D}^*$ is a diagonal matrix with the inverted, non-negative singular values of **D**. But given that the last ($P{-}D{+}1$) singular values are zero, one can take only the first $k=D{-}1$ (the non-zero ones) and their associated left and right singular vectors, in some *reduced matrices* $\mathbf{V}_k$, $\mathbf{D}_k$ and $\mathbf{U}_k$, as in Eckart and Young (1936) approximation of one matrix by another of lower rank, to obtain

$$\mathbf{y}_0 = \mathbf{x} \cdot \mathbf{A}^* = \mathbf{x} \cdot (\mathbf{V}_k \cdot \mathbf{D}_k^{-1} \cdot \mathbf{U}_k^t).$$

2. If no component of $\mathbf{y}_0$ is negative, we found a valid solution: do not continue with the next steps.

3. If some components of $\mathbf{y}_0$ are negative, one has to look for a valid solution. From the left singular vectors, take the last ($P{-}D{+}1$), those corresponding to zero singular values. Denote them by $\mathbf{u}_i$, and the selected columns organized in a matrix as $\mathbf{U}^0$. These vectors form a basis spanning the subspace of the mineral compositions that are solutions of Equation (2). Thus all possible solutions can be written as

$$\mathbf{y} = \mathbf{y}_0 + \Sigma^P_{i=D} \lambda_i \cdot \mathbf{u}_i = \mathbf{y}_0 + \lambda \cdot \mathbf{U}_0,$$

with some unknown $\lambda=[\lambda_D, \lambda_{D+1},..., \lambda_P]$.

4.With standard quadratic programming routines, look for the vector λ such that

- the norm $||\mathbf{y}||$ is minimal; given that $\mathbf{y}_0$ is by construction a linear combination of the first $(D–1)$ columns of $\mathbf{U}$, it is orthogonal to the columns of $\mathbf{U}_0$ and therefore Pythagoras Theorem applies, which gives $||\mathbf{y}||^2=||\mathbf{y}_0||^2+||\lambda||^2$; since $\mathbf{y}_0$ is fixed, minimizing $\mathbf{y}$ is equivalent to minimizing λ (or its square), which is the typical option implemented in quadratic programming algorithms (e.g. *quadprog* in *R*);
- all components of $\mathbf{y}$ are positive, which is equivalent to force $\mathbf{y}_0 \geq \lambda \cdot \mathbf{U}_0$, an inequality to be read by components.

Note that the condition of minimal norm, given that $\mathbf{y}$ sums up to one, promotes compositions with many non-zero components. For this reason, the method can overestimate the number of endmember present. Or better said, it will result in a null contribution of a mineral only when it does not fit by any means in the observed geochemical composition.

A.2   Results

The following minerals are considered as end-members (i.e., matrix $\mathbf{A}^t$):

	SiO_2	Al_2O_3	Fe_2O_3	MgO	MnO	CaO	Na_2O	K_2O	P_2O_5
qz	1	0	0	0	0	0	0	0	0
alb	3	0.5	0	0	0	0	0.5	0	0
ano	2	1	0	0	0	1	0	0	0
kfs	3	0.5	0	0	0	0	0	0.5	0
phl	3	0.5	0	3	0	0	0	0.5	0
alm	3	1	3	0	0	0	0	0	0
epi	3	1	0.5	0	0	1	0	0	0
sps	3	1	0	0	6	0	0	0	0
apa	0	0	0	0	0	5	0	0	1.5
mus	3	1.5	0	0	0	0	0	0.5	0
bio	3	0.5	1.5	0	0	0	0	0.5	0
prp	3	1	0	6	0	0	0	0	0
clz	3	1.5	0	0	0	2	0	0	0
fcl	5.67	2.67	4.5	0	0	0	0	0	0
mcl	5.67	2.67	0	9	0	0	0	0	0
molar weights	60	102	160	40.3	71	56	62	94.2	142

Looking at Figure 6, it is interesting to note that the mineral composition for the coarsest grain fractions is quite constant, as was the geochemistry (Figures 1 and 3). Also, muscovite is barely present in the sand fraction: the computations suggest that this mica is present in the coarser grains, within rock fragments, and reappears again in the silt fraction ($\phi > 5$). Biotite, contrarily, is present in all fractions. In general the proportions of all phyllosilicates tend to increase in the finer fractions, though this does not seem to happen at the expense of feldspar, but of quartz. Assuming the computations correct, this feldspar permanence is an argument against the presence of a significant weathering: quartz would decrease in the finer fractions simply because it cannot easily be further comminuted beyond the silt spectrum, whereas phyllosilicates can easily break down, being more feasible than the rest. Chemical weathering would thus again become unnecessary.
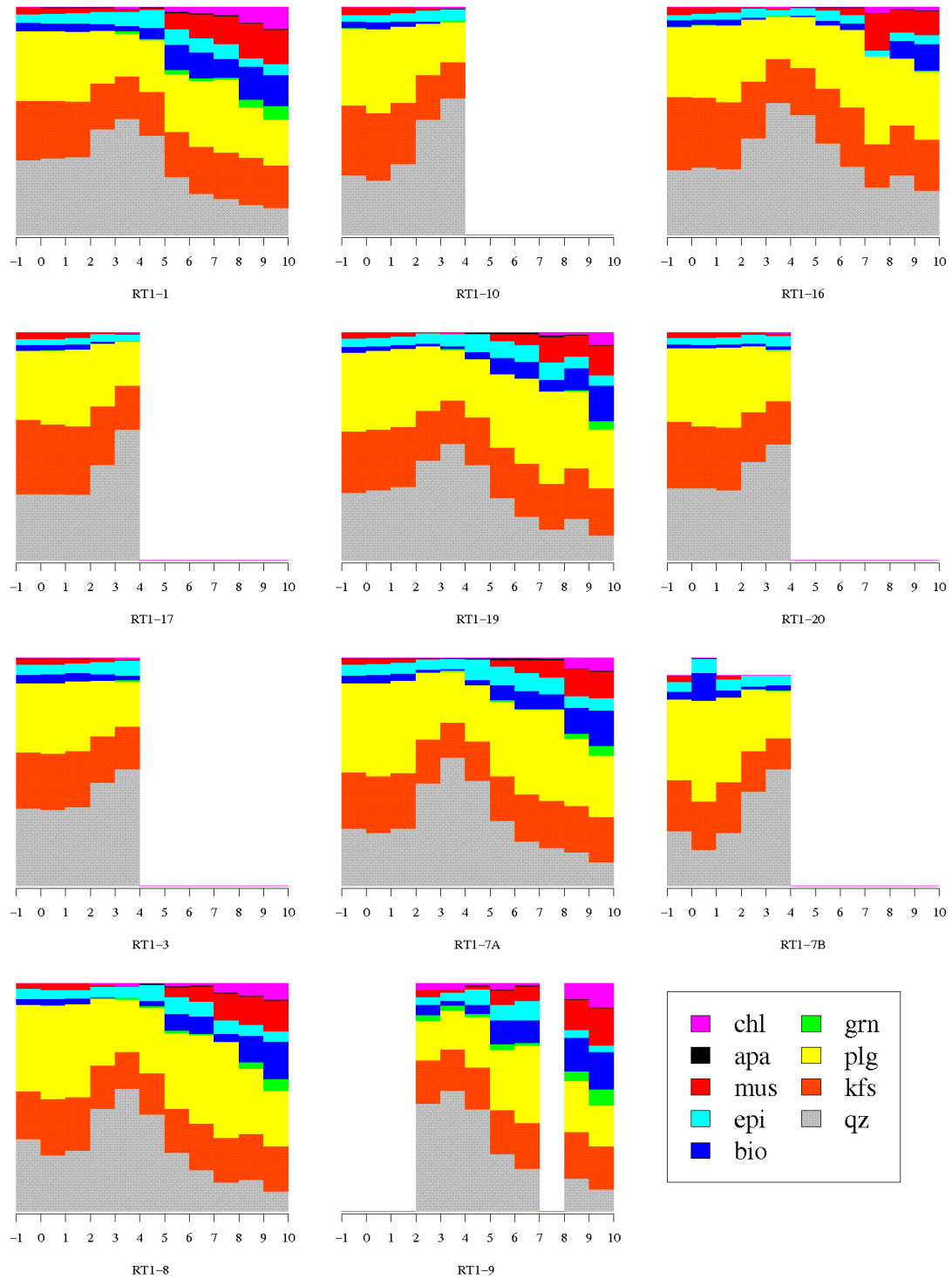
Figure 6: Bar plots of the mineral composition obtained by considering the main endmember minerals of granites (quartz, several feldspars, biotite, garnet, apatite). The bar not summing up to 1 has negative components, thus the end-member model is not admissible for it (either due to badly characterized geochemitstry or because an important mineral was not considered).

Table 2: Statistics of the (absolute) negative values of the computed mineralogical composition: the first part of the table reports results from the first attempt, step 2, whereas the second part give results obtained in the refinement process of steps 3-5.

| mineral	number	Min.	1st Qu.	Median	Mean	3rd Qu.	Max.
phl	5	0.0225	0.0028	0.0026	0.0060	0.0014	0.0006
alm	66	0.0199	0.0117	0.0088	0.0087	0.0049	0.0004
mus	7	0.0338	0.0162	0.0120	0.0148	0.0088	0.0077
bio	7	0.0407	0.0098	0.0087	0.0109	0.0037	0.0002
prp	40	0.0130	0.0079	0.0042	0.0056	0.0029	0.0003
clz	52	0.0522	0.0195	0.0092	0.0132	0.0048	0.0008
fcl	61	0.0364	0.0112	0.0084	0.0087	0.0040	0.0004
mcl	40	0.0238	0.0079	0.0050	0.0062	0.0037	0.0000
alm	1	0.0094	0.0094	0.0094	0.0094	0.0094	0.0094
mus	1	0.0086	0.0086	0.0086	0.0086	0.0086	0.0086
bio	1	0.0000	0.0000	0.0000	0.0000	0.0000	0.0000
prp	1	0.0029	0.0029	0.0029	0.0029	0.0029	0.0029
fcl	1	0.0364	0.0364	0.0364	0.0364	0.0364	0.0364
mcl	1	0.0238	0.0238	0.0238	0.0238	0.0238	0.0238
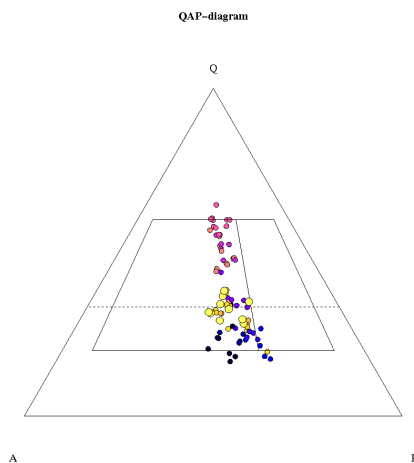
Figure 7: Upper half of the Streckeisen diagram, showing that the calculated quartz-plagioclase-K feldspar compositions correspond to typical granodioritic compositions (note: albite was considered to be 80% in plagioclase and 20% in K-feldspar). This is particularly clear for the coarse to medium grain fractions (the coarsest showed with bigger symbols). Fine sand to coarse silt fractions are enriched in quartz, and the finest fractions are depleted in quartz. A dashed line shows the range of feldspar/quartz ratios from the Aar Massif granitoids reported by Debon and Lemmet (1999).

Figure 7 casts some light on this problem, by showing where do the computed mineral compositions plot in several reference diagrams. It shows that the bulk rock should correspond to a granodiorite (as plotted in the Streckeisen diagram), and that grain size does not modifies in the relation plagioclase/alkali feldspar: only quartz varies. If weathering was active, one should expect some loss of plagioclase with respect to alkali feldspar, and this is not observed (only very slighlty in the finest fraction).